IOSR Journal of Applied Physics (IOSR-JAP)
e-ISSN: 2278-4861.Volume 17, Issue 2 Ser. 1 (Mar. – Apr. 2025), PP 41-47
www.iosrjournals.org

Spectral and Raman Analysis of Tb^{3+} doped Yttrium Zinc Lithium Cesium Barium Bismuth Borate Glasses

S.L.Meena
Ceremic Laboratory, Department of physics, Jai Narain Vyas University, Jodhpur 342001(Raj.) India
E-mail address:shankardiya7@rediffmail.com

Abstract
Glass sample of Yttrium Zinc Lithium Cesium Barium Bismuth Borate Glasses (35-x) Bi_2O_3 :10ZnO :10Li_2O :10Cs_2O_3 :10BaO : 10Y_2O_3:15B_2O_3:xTb_2O_3. (where x=1,1.5,2 mol%) have been prepared by melt-quenching technique. The amorphous nature of the prepared glass samples was confirmed by X-ray diffraction. The absorption, fluorescence and raman spectra of three Eu^{3+} doped zinc lithium cadmium magnesium bismuth borate glasses have been recorded at room temperature. The various interaction parameters like Slater-Condon parameters F_k (k=2,4,6), Lande' parameter (ξ_{4f}), nephelauexetic ratio (β'),bonding parameter ($b^{1/2}$)and Racah parameters E^k(k=1,2 3) have been computed. Judd-Ofelt intensity parameters and laser parameters have also been calculated.

Keywords: *YZLCBBB glasses, Energy interaction parameters, Optical properties, Raman analysis.*

Date of Submission: 05-03-2025 Date of Acceptance: 17-03-2025

I. Introduction

Glasses with dopants of rare earth ions have continuously drawn the attention through their potential applications in optical Amplifiers, solid state lasers, solid state batteries, sensing laser technology and sensor fields [1-5]. Bismuth borate glasses doped with a transition metal or rare-earth ions are considered as valuable materials for both optical and electrical applications. The high gain density in borate glasses is due to high solubility of rare earth ions in borate network. These characteristics are known to have some influences on various factors such as the preparation temperature, nature and the composite type. The addition of Li_2O improves the physical and chemical properties of the glass [6-9]. ZnO is a wide band gap semiconductor and has received increasing research interest. It is an important multifunctional material due to its specific chemical, surface and micro structural properties [10, 11].Due to their good chemical durability, terbium -doped borate glasses are attractive materials for the fabrication of low-cost integrated optical amplifiers by using the ion-exchange technique. Glasses contain B_2O_3 have received increased attention due to their application in the field of glass ceramics, reflecting windows, thermal and mechanical sensors [12-15].There are several reported works on the structural, spectral and luminescence properties of Tb^{3+} ions in various silicate glasses [16-19].Recently borate based glasses have a wide range of potential applications in optical data transmission, sensing, energy solar cell and laser technologies [20, 21].

The aim of the present study is to prepare the Tb^{3+} doped yttrium zinc lithium cesium barium bismuth borate glass with different Tb_2O_3 concentrations. The absorption, fluorescence and raman spectra of $Tb^{3+}$of the glasses were investigated. The Judd-Ofelt theory has been applied to compute the intensity parameters Ω_λ (λ=2, 4, 6).These intensity parameter have been used to evaluate optical optical properties such as spontaneous emission probability, branching ratio, radiative life time and stimulated emission cross section.

II. Experimental Techniques

Preparation of glasses

The following Tb^{3+} doped bismuth borate glass samples (35-x) Bi_2O_3 :10ZnO :10Li_2O :10Cs_2O_3 :10BaO : 10Y_2O_3:15B_2O_3:xTb_2O_3. (where x=1,1.5, 2) have been prepared by melt-quenching method. Analytical reagent grade chemical used in the present study consist of Bi_2O_3, ZnO, Li_2O,Cs_2O_3, BaO,Y_2O_3, $B_2O_3$and Tb_2O_3. They were thoroughly mixed by using an agate pestle mortar. then melted at 960^0C by an electrical muffle furnace for 2h., After complete melting, the melts were quickly poured in to a preheated stainless steel mould and annealed at temperature of 250^0C for 2h to remove thermal strains and stresses. Every time fine powder of cerium oxide was used for polishing the samples. The glass samples so prepared were of good optical quality and were transparent. The chemical compositions of the glasses with the name of samples are summarized in Table 1.

Table 1

Chemical composition of the glasses

Sample	Glass composition (mol %)
YZLCBBB (UD)	$40P_2O_5$:10ZnO:$10Li_2O$:10CdO:10MgO:$20B_2O_3$
YZLCBBB (TB1)	$39P_2O_5$:10ZnO:$10Li_2O$:10CdO:10MgO:$20B_2O_3$: 1 Tb_2O_3
YZLCBBB (TB 1.5)	$38.5P_2O_5$:10ZnO:$10Li_2O$:10CdO:10MgO:$20B_2O_3$: 1.5 Tb_2O_3
YZLCBBB (TB 2)	$38P_2O_5$:10ZnO:$10Li_2O$:10CdO:10MgO:$20B_2O_3$: 2 Tb_2O_3

YZLCBBB (UD) -Represents undoped Yttrium Zinc Lithium Cesium Barium Bismuth Borate glass specimen.
YZLCBBB (TB) -Represents Tb^{3+} doped Yttrium Zinc Lithium Cesium Barium Bismuth Borate glass specimens.

III. Theory

3.1 Oscillator Strength

The spectral intensity is expressed in terms of oscillator strengths using the relation [22].

$$f_{expt.} = 4.318 \times 10^{-9} \int \varepsilon(\nu)\, d\nu \qquad (1)$$

Where, $\varepsilon(\nu)$ is molar absorption coefficient at a given energy ν (cm^{-1}), to be evaluated from Beer–Lambert law. Under Gaussian Approximation, using Beer–Lambert law, the observed oscillator strengths of the absorption bands have been experimentally calculated [23], using the modified relation:

$$P_m = 4.6 \times 10^{-9} \times \frac{1}{cl} \log \frac{I_0}{I} \times \Delta\upsilon_{1/2} \qquad (2)$$

Where c is the molar concentration of the absorbing ion per unit volume, l is the optical path length, $\log I_0/I$ is optical density and $\Delta\upsilon_{1/2}$ is half band width.

3.2. Judd-Ofelt Intensity Parameters

According to Judd [24] and Ofelt [25] theory, independently derived expression for the oscillator strength of the induced forced electric dipole transitions between an initial J manifold $|4f^N (S, L) J\rangle$ level and the terminal J' manifold $|4f^N (S',L') J'\rangle$ is given by:

$$\frac{8\Pi^2 mc\bar{\upsilon}}{3h(2J+1)} \frac{1}{n}\left[\frac{(n^2+2)^2}{9}\right] \times S(J, J') \qquad (3)$$

Where, the line strength S (J, J') is given by the equation

$$S(J, J') = e^2 \sum_{\lambda=2,4,6} \Omega_\lambda \langle 4f^N (S, L) J \| U^{(\lambda)} \| 4f^N (S', L') J' \rangle^2$$

In the above equation m is the mass of an electron, c is the velocity of light, ν is the wave number of the transition, h is Planck's constant, n is the refractive index, J and J' are the total angular momentum of the initial and final level respectively, Ω_λ ($\lambda = 2, 4, 6$) are known as Judd-Ofelt intensity parameters.

3.3 Radiative Properties

The Ω_λ parameters obtained using the absorption spectral results have been used to predict radiative properties such as spontaneous emission probability (A) and radiative life time (τ_R), and laser parameters like fluorescence branching ratio (β_R) and stimulated emission cross section (σ_p).

The spontaneous emission probability from initial manifold $|4f^N (S', L') J'\rangle$ to a final manifold $|4f^N (S, L) J\rangle$ is given by:

$$A[(S', L') J'; (S, L) J] = \frac{64\pi^2\nu^3}{3h(2J'+1)}\left[\frac{n(n^2+2)^2}{9}\right] \times S(J', \bar{J}) \qquad (4)$$

Where, $S(J', J) = e^2 [\Omega_2 \| U^{(2)} \|^2 + \Omega_4 \| U^{(4)} \|^2 + \Omega_6 \| U^{(6)} \|^2]$

The fluorescence branching ratio for the transitions originating from a specific initial manifold $|4f^N (S', L') J'\rangle$ to a final many fold $|4f^N (S, L) J\rangle$ is given by

$$\beta[(S', L')\ J';\ (S, L)\ J] = \sum_{S\ L\ J} \frac{A[(S'\ L')]}{A[(S'\ L')\ J'(\bar{S}\ \bar{L})]} \qquad (5)$$

Where, the sum is over all terminal manifolds.

The radiative life time is given by

$$\tau_{rad} = \sum_{S\ L\ J} A[(S', L')\ J';\ (S, L)] = A_{Total}^{-1} \qquad (6)$$

Where, the sum is over all possible terminal manifolds. The stimulated emission cross -section for a transition from an initial manifold $|4f^N (S', L')\ J'>$ to a final manifold $|4f^N (S, L)\ J>|$ is expressed as

$$\sigma_p(\lambda_p) = \left[\frac{\lambda_p^4}{8\pi c n^2 \Delta\lambda_{eff}}\right] \times A[(S', L')\ J';\ (\bar{S}, \bar{L})\bar{J}] \qquad (7)$$

Where, λ_p the peak fluorescence wavelength of the emission band and $\Delta\lambda_{eff}$ is the effective fluorescence line width.

3.4 Nephelauxetic Ratio (β) and Bonding Parameter ($b^{1/2}$)

The nature of the R-O bond is known by the Nephelauxetic Ratio (β') and Bonding Parameter ($b^{1/2}$), which are computed by using following formulae [26, 27]. The Nephelauxetic Ratio is given by

$$\beta' = \frac{\nu_g}{\nu_a} \qquad (8)$$

where, ν_g and ν_a refer to the energies of the corresponding transition in the glass and free ion, respectively. The values of bonding parameter ($b^{1/2}$) is given by

$$b^{1/2} = \left[\frac{1-\beta'}{2}\right]^{1/2} \qquad (9)$$

IV. Result and Discussion

4.1 XRD Measurement

Figure 1 presents the XRD pattern of the sample contain - B_2O_3 which is show no sharp Bragg's peak, but only a broad diffuse hump around low angle region. This is the clear indication of amorphous nature within the resolution limit of XRD instrument.

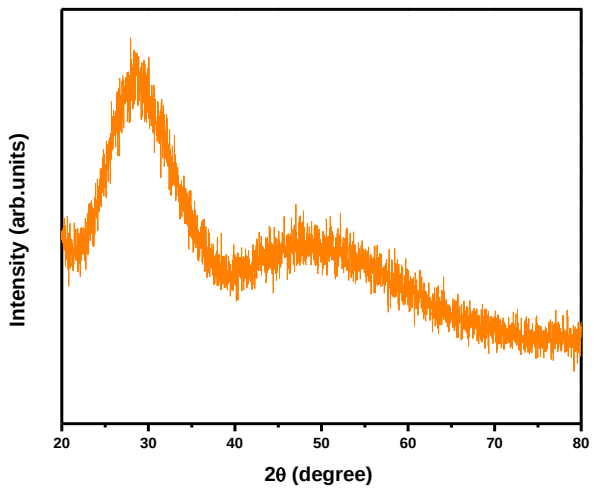

Fig.1: X-ray diffraction pattern of YZLCBBB TB (01) glass.

4.2 Raman spectra

The Raman spectrum of Yttrium Zinc Lithium Cesium Barium Bismuth Borate YZLCBBB TB (01) glass specimen is recorded and is shown in Fig. 2. The spectrum peaks located at 445, 746, 985 and 1276 cm^{-1}.The band at 445 $cm^{-1}$is assigned to vibrations of Bi–O–Bi band of BiO_6 octahedral units. The band at 746 $cm^{-1}$is due to vibrations of metaborate group. The band at 985 $cm^{-1}$is due to vibrations of orthoborate groups. The bands at 1276 cm^{-1} is due to the B–O stretching vibrations.

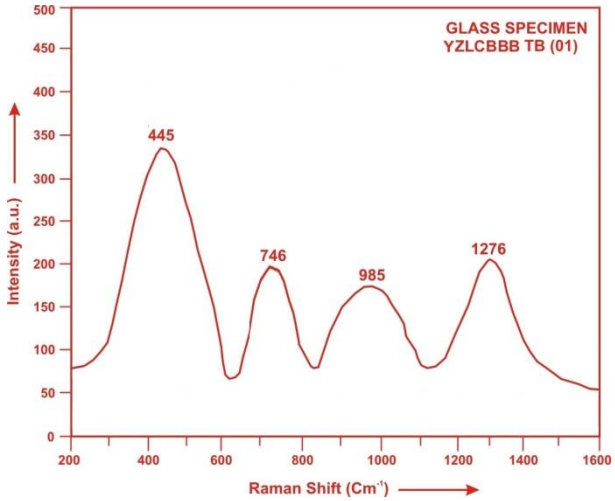

Fig.2: Raman spectrum of YZLCBBB TB (01) glass.

4.3 Absorption Spectrum

The absorption spectra of Tb^{3+} doped YZLCBBB (TB 01) glass specimen has been presented in Figure 3 in terms of optical density versus wavelength (nm). Five absorption bands have been observed from the ground state $^7F_6$ to excited states $^5D_4$,$^5D_3$,$^5L_{10}$, $^5D_2$ and $^5L_9$ for Tb^{3+}doped YZLCBBB TB (01) glass.

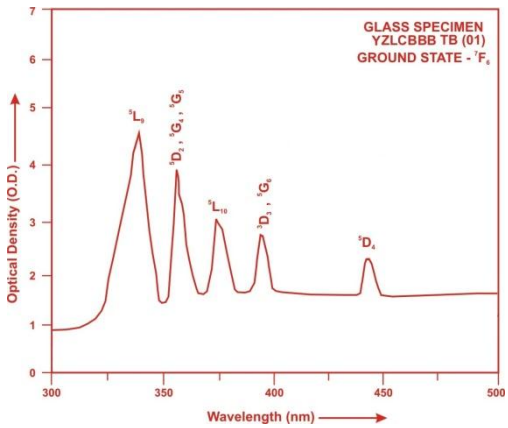

Fig.3: Absorption spectrum of YZLCBBB **TB (01) glass.**

The experimental and calculated oscillator strengths for Tb^{3+}ions in yttrium zinc lithium cesium barium bismuth borate glasses are given in Table 2.

Table2: Measured and calculated oscillator strength ($P_m \times 10^{+6}$) of Tb^{3+}ions in YZLCBBB glasses.

Energy level $^7F_0$	**Glass YZLCBBB (TB01)**		**Glass YZLCBBB (TB1.5)**		**Glass YZLCBBB (TB02)**	
	$P_{exp.}$	$P_{cal.}$	$P_{exp.}$	$P_{cal.}$	$P_{exp.}$	$P_{cal.}$
$^5D_4$	0.56	0.08	0.54	0.07	0.51	0.08
$^5D_3$	0.91	0.45	0.87	0.43	0.85	0.45
$^5L_{10}$	1.64	1.23	1.62	1.22	1.60	1.25
$^5D_2$	1.92	0.64	1.89	0.62	1.86	0.65
$^5L_9$	2.19	1.08	2.17	1.07	2.14	1.10
r.m.s. deviation	0.83653		0.82427		0.77752	

The small value of r.m.s. deviation indicates fairness of fitting between experimental and calculated oscillator strengths.

Computed values of F_2, Lande' parameter (ξ_{4f}), Nephlauxetic ratio (β') and bonding parameter($b^{1/2}$) for Tb^{3+}doped YZLCBBB glass specimen are given in Table 3.

Table 3. F_2, ξ_{4f}, β' and $b^{1/2}$ parameters for Terbium doped glass specimen.

Glass Specimen	F_2	ξ_{4f}	β'	$b^{1/2}$
Tb^{3+}	400.26	1820.87	0.9703	0.1219

In the present case the three Ω_λ parameters follow the trend $\Omega_2 > \Omega_6 > \Omega_4$. The spectroscopic quality factor (Ω_4/Ω_6) related with the rigidity of the glass system has been found to lie between 0.479 and 0.813 in the present glasses.

The value of Judd-Ofelt intensity parameters are given in **Table 4**

Table4: Judd-Ofelt intensity parameters for Tb^{3+} doped ZLCBBB glass specimens.

Glass Specimen	**Ω_2(pm^2)**	**Ω_4(pm^2)**	**Ω_6(pm^2)**	**Ω_4/Ω_6**	**Trend**	**References**
YZLCBBB (TB01)	8.475	2.279	2.804	0.813	**$\Omega_2 > \Omega_6 > \Omega_4$**	P.W.
YZLCBBB (TB1.5)	7.216	2.045	2.796	0.732	**$\Omega_2 > \Omega_6 > \Omega_4$**	P.W.
YZLCBBB (TB02)	8.419	2.245	2.857	0.786	**$\Omega_2 > \Omega_6 > \Omega_4$**	P.W.
LLBP(TB)	3.339	1.179	2.462	0.479	**$\Omega_2 > \Omega_6 > \Omega_4$**	[28]

4.4 Excitation Spectrum

Excitation spectra of YZLCBBB TB (01) glass recorded at the emission wavelength 544 nm is depicted as figure 4. The excitation spectra was recorded in the spectral region 300-550nm fluorescence at 544 nm having different excitation band centered at 305,316,331,345,359,368,377,386 and 484 are attributed to the $^5H_6$,$^5H_7$,$^5D_1$,$^5L_7$+$^5L_8$,$^5L_9$,$^5G_5$,$^5L_{10}$,$^5D_3$+$^5G_6$ and $^5D_4$ transitions respectively. The highest absorption level is $^5D_3$+$^5G_6$ and is at 386 nm. So this is to be chosen for excitation wavelength.

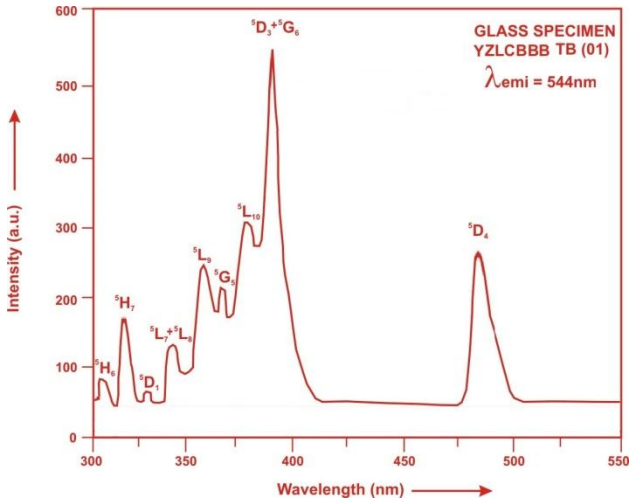

Fig.4: Excitation spectrum of YZLCBBB TB (01) glass.

4.4. Fluorescence Spectrum

The fluorescence spectrum of Tb^{3+}doped in yttrium zinc lithium cesium barium bismuth borate glass is shown in Figure 5. There are four broad bands observed in the Fluorescence spectrum of Tb^{3+}doped yttrium zinc lithium cesium barium bismuth borate glass. The wavelengths of these bands along with their assignments are given in Table 5. Fig.(5).Shows the fluorescence spectrum with four peaks ($^5D_4 \rightarrow {}^7F_6$), ($^5D_4 \rightarrow {}^7F_5$), ($^5D_4 \rightarrow {}^7F_4$) and ($^5D_4 \rightarrow {}^7F_3$) for glass specimens.

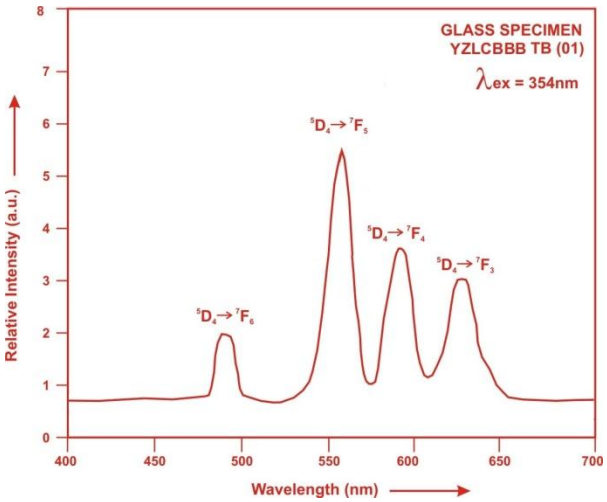

Fig.5: Fluorescence spectrum of YZLCBBB TB (01) glass.

Table5. Emission peak wave lengths (λ_{max}),radiative transition probability (A_{rad}),branching ratio (β),stimulated emission cross-section(σ_p) and radiative life time(τ_R) for various transitions in Tb^{3+}doped YZLCBBB glasses.

Transition		YZLCBBB (TB 01)				YZLCBBB (TB 1.5)				YZLCBBB (TB 02)			
	λ_{max} (nm)	$A_{rad}(s^{-1})$	β	σ_p (10^{-20} cm^2)	$\tau_R(\mu s)$	$A_{rad}(s^{-1})$	β	σ (10^{-20} cm^2)	$\tau_R(\mu s)$	$A_{rad}(s^{-1})$	β	σ_p (10^{-20} cm^2)	$\tau_R(\mu s)$
$^5D_4 \rightarrow {}^7F_6$	488	2974.69	0.0933	0.4794		2673.75	0.0965	0.4253		2983.91	0.0937	0.4658	
$^5D_4 \rightarrow {}^7F_5$	550	22703.60	0.7124	1.8214		19556.90	0.7057	3.2500		22668.00	0.7118	3.7339	
$^5D_4 \rightarrow {}^7F_4$	582	1979.14	0.0621	0.7381	31.38	1831.92	0.0661	0.6732	36.08	1984.80	0.06233	0.7140	31.40
$^5D_4 \rightarrow {}^7F_3$	625	4213.95	0.1322	1.1602		3652.12	0.1318	0.9930		4209.18	0.1322	1.1346	

V. Conclusion

In the present study, the glass samples of composition (35-x) Bi_2O_3 :10ZnO :10Li_2O :10Cs_2O_3 :10BaO : 10Y_2O_3:15B_2O_3:xTb_2O_3. (where x=1, 1.5, 2mol %) have been prepared by melt-quenching method. The Judd-Ofelt theory has been applied to calculate the oscillator strength and intensity parameters Ω_λ (λ=2, 4, 6). The radiative transition rate and the branching ratio are highest for ($^5D_4 \rightarrow {}^7F_5$) transition and hence it is useful for laser action. The stimulated emission cross section (σ_p) value is also very high for the transition ($^5D_4 \rightarrow {}^7F_5$). This shows that ($^5D_4 \rightarrow {}^7F_5$) transition is most probable transition.

References

[1]. Meena, S.L.(2024).Photoluminescence and Raman analysis of Nd^{3+} doped in ytterbium zinc lithium sodium barium calcium aluminophosphate glasses, IOSR Appl.Phys.16,28-34.

[2]. Boudchicha,N.,Iezid,M.,Goumeidane,F.,Legouera,M.,Prasad,P.S.,Rao,P.V.(2023).Judd–Ofelt Analysis and Spectroscopy Study of Tellurite Glasses Doped with Rare-Earth (Nd^{3+}, Sm^{3+}, Dy^{3+}, and Er^{3+}),Materials,16,6832,1-19.

[3]. De, M.,Jana, S.(2020).Optical characterization of Eu^{3+} doped titanium barium lead phosphate glass, Optik-Int. Journal for light and Electron Optics,215,164718,1-7.

[4]. Mirdda,J.N., Mukhopadhyay,S.,Sahu,K.R.,Goswami,M.N.(2020). Enhancement of optical emission and dielectric properties of Eu^{3+}-doped Na_2O–ZnO–TeO_2 glass material, Glass Phys. Chem. 46,218-227.

[5]. Meena,S.L.(2024).Spectral and Thermal properties of Tm^{3+} doped in zinc lithium tungsten antimony borophosphate glasses,IOSR Appl.Phys.16,10-15.

[6]. Monisha, M., Nancy, A., Souza, D., legde, V., Prabhu, N.S. and Sayyed, M.I.(2020). Dy^{3+} doped SiO_2- B_2O_3-Al_2O_3-NaF-ZnF_2 glasses : An exploration of optical and gamma radiation shielding features, Current Applied Physics 20(11), 1207-1210.

[7]. Anjaiah, J. and Laxmikanth, C. (2015). Optical Properties of Neodymium Ion Doped Lithium Borate Glasses, 5,173 -183.

[8]. Pawar, P.P., Munishwar, S.R. and Gedam, R.S. (2017). Intense white light luminescent Dy^{3+} doped lithium borate glasses for WLED: a correlation between physical, thermal, structural and optical properties. Solid State Sci., 64, 41–50.

[9]. Rani.P.R.,Venkateswarlu,M.,Swapna,K.,Mahamuda,Sk.,Srinivas Prasad,M.V.V.K.,Rao,A.S.(2020).Spectroscopic and luminescence properties of Ho^{3+} ions doped barium lead alumino fluoro borate glasses for green laser applications,Solid State Sci.102,106175.

[10]. Pavani, P. G., Sadhana, K., Mouli, V. C. (2011).Optical, physical and structural studies of boro-zinc tellurite glasses, Physica B: Condensed Matter, 406, 1242–1247.

[11]. Pal, M., Roy, B.and Pal, M. (2011). Structural characterization of borate glasses containing zinc and manganese oxide. J.Mod.Physics, 2, 1062-66.

[12]. Kotab,I.E.,Okasha,S.Y.,Zidan,N.A.(2023).Extensive study on the optrical and structural characteristics of Nd^{3+} doped lead-borate-strontium-tungsten glass system.Judd-Ofelt Anal.Res.Chem.5,1-12.

[13]. Xia,Y.J.P,Zhang,T.(2024).Advances in the optical and electronic properties and applications of bismuth based semiconductor materials,J.Mat.Chem. C 12,1609-1624.
[14]. Basappa,A.T.N.,Kolavekar,S.B.,Sathish,K.N.,Shashidhar,S.,Keshavamurthy,K.(2024).Effect of silver nanoparticle size on the ultrafast optical nonlinear and optical limiting properties of Nd^{3+} doped antimony borate glasses,Inf.Phys.Tech.138,105268.
[15]. Meena,S.L.(2020).Spectroscopic properties of Er^{3+} doped zinc lithium arsenic strontium vanadium bismuth borate glasses,IOSR Appl.Phys.12,05-10.
[16]. Vijayasri,Rudramamba,K.S.,Srikanth,T.,Reddy,N.M.,Nahha,M.,Pratyusha,S.,Reddy,M.R.(2023).Spectroscopic features of Tb^{3+} doped strontium zinc borate glasses for green laser applications,J.Mol.Struct.1274(3),134514
[17]. Zheng,J., Wu,X., Ren,Q., Ren,Y., Hai,Q.(2020).Luminescence properties, energy transfer and thermal stability of blue-green color tunable $Sr_3Y(BO_3)_3:Ce^{3+},Tb^{3+}$ phosphors, Opt. Laser Tech.123,105900.
[18]. Dhinakaran,A.P.,Vinothkumar,P.Senthil,T.S.,Kalpana,S.(2024). Investigation on luminescent characteristics of Tb^{3+}/Dy^{3+} co-doped borophosphate glass for cool white LED and radiation shielding applications, Appl.Phys.A,130,709
[19]. Kochanowicz,M.,Dorosz,D.,Zmojda,J.,Dorosz,J.,Pisarska,J.Pisarski,W.A.(2014). Up-conversion luminescence of Tb^{3+} ions in germinate glasses under diode-laser excitation of Yb3+, Opt.Mat.Exp.4, 1050-1056.
[20]. Sailaja,P.,Mahamuda,Sk.,Dedeepya,G.,Alzahrani,J.S.,Swapna,K.,Venkateswarlu,M.,Rao,A.S.,Alrowaili,Z.A.,Olarinoye,I.O.,Al-Buriahi,M.S.(2024).Effect of Eu^{3+} ions concentration on visible red luminescence and radiative shielding properties of $SrO-Al_2O_3-BaCl_2-B_2O_3-TeO_2$ glasses,Rad.Phys.Chem.216,111467.
[21]. Kumar,B.N.S.,Devaraja,C.,Gedam,R.S.,Eraiah,B.,G.G.V.Jagadeesha,Harisha,G.,R.G.V.Ashok,Implications of silver nitrate doping on the physical, structural and optical attributes of Na_2O-ZnO-Borate glasses,J.MOL.Struct.1325,140985.
[22]. Gorller-Walrand, C. and Binnemans, K. (1988). Spectral Intensities of f-f Transition. In: Gshneidner Jr., K.A. and Eyring,L., Eds., Handbook on the Physics and Chemistry of Rare Earths, Vol. 25, Chap. 167, North-Holland, Amsterdam, 101-264.
[23]. Meena,S.L.(2024).Spectral and Luminescence Study of Er^{3+} Doped Phosphate Glasses for the Development of 1.5 μm Broadband Amplifier, IOSR Appl.Phys.35-41.
[24]. Judd, B.R.(1962).Optical absorption intensities of rare earth ions,Phys.Rev.127,750-761.
[25]. Ofelt,G.S. (1962). Intensities of crystal spectra of rare earth Ions, Chem.Phys37, 511-520.
[26]. Sinha, S.P. (1983). Systematics and properties of lanthanides, Reidel, Dordrecht.
[27]. Krupke, W.F. (1974).IEEE J. Quantum Electron QE, 10,450
[28]. Meena,S.L.(2018).Spectral and Thermal properties of Tb^{3+} doped in lead lithium borophosphate glasses,Int.Cem.Phys.Sci.7,1-8.